Kinetic Study and Reaction Mechanism of Vinyl Monomer Modified *Antheraea assama* Silk Composites

A. M. Das*

North East Institute of Science & Technology, Jorhat 785 006, Assam, India

A biodegradable protein fiber *Antheraea assama* silk (SH) was modified by using graft co-polymerization technique with methyl methacrylate (MMA; vinyl monomer) and cerric ammonium sulfate (Ce^{IV}). The grafting process was dependent on MMA, Ce^{IV}, time factors, temperatures and other properties of the fibroin composites. The possible mechanism of the SHMMA composite was explained by free radical co-polymerization, and the thermal properties were characterized by thermogravimetric analysis (TGA), differential thermogravimetry (DTG), differential thermal analysis (DTA), and differential scanning calorimetry (DSC). The kinetic parameters were also studied using the Coats and Redfern method with FORTRAN 77 computer programming and evaluating the activation energy. The structural changes of SHMMA, changes of the crystalline and amorphous characteristics after chemical process with MMA−Ce^{IV} initiator, were discussed in relation to the weight gain and X-ray diffraction curves. This study shows that silk fibroin composites modified by graft co-polymerization have improved thermal stability and chemical stability, which improve the drawbacks and make the silk fibroin a promising material in constructing textiles.

Introduction

The use of natural fibers at the industrial level improves the environmental sustainability of the parts being constructed, especially within the automotive market. Modification of natural or synthetic fibroin with the aim of imparting specific properties to the products has given a great thrust to macromolecular/polymer science/textile chemistry. Desirable and targeted properties can be imparted to the natural or synthetic fibroin through graft co-polymerization in order to mete-out the requirement of specialized applications. It is a convenient and clean means for altering the properties of numerous polymer backbones and provides a number of new advantageous properties.[1] *Antheraea assama* (*A. assama*) silk fibroin is a well-described natural protein fiber produced by the silkworm *A. assama* Westwood (Lepidoptera: Saturniidae), a multivoltine, sericogenic insect native to North Eastern India,[2] which has been used traditionally in the form of thread in textiles for thousands of years. The silk contains a fibrous protein that forms the thread core and a gluelike protein, termed sericin, that surrounds the fibroin and cements them to together.[3] Recent interest lies on the application of silk fibroin (SH) as the biomaterials because of its unique mechanical properties as well as its biocompatibility and biodegradability.[4] *A. assama* SH composites are excellent clothing materials with outstanding mechanical and aesthetic characteristics which are exploited for production of precious textile goods.

Recently, electrospinning using natural proteins and synthetic polymers offers an attractive technique for producing fibrous scaffolds with potential for tissue regeneration and repair. Nanofibrous scaffolds of silk fibroin (SF) and poly(L-lactic acid-*co*-epsilon-caprolactone) {P(LLA-CL)} blends were fabricated using 1,1,1,3,3,3-hexafluoro-2-propanol as a solvent via electrospinning and also scaffold, blending the silk fibroin with other natural or synthetic polymers, such as P(LLA-CL),[5] *N*-methylmorpholine *N*-oxide hydrates (NMMO/H_2O),[6] chitosan,[7] PLA,[8] collagen,[9] and poly(ethylene oxide) (PEO),[10] etc. Recently, extensive research has been conducted on scientific and industrial applications of hydrophobic silica nanoparticles and gold nanoparticles to hydrophilic fabrics to realize superhydrophobic textiles with self-cleaning properties by many approaches.[11] The interpretation of polymerization kinetics demands knowledge of reliable kinetic parameters. They provide the basis for more accurate design of the polymerization reaction mechanism and better insight into the behavior of existing reactions; although the literature contains an abundance of initiator decomposition rates in various solvents of in situ rate, data for polymerization systems are scarce.[12]

This variety of silk has some drawbacks such as photoyellowing, wrinkle recovery, and abrasion resistance, etc. So, we have tried to improve these drawbacks by applying a graft co-polymerization technique.

In the present paper we discuss the mode of free radical reaction mechanism in the formation of SHMMA composites with the thermal properties of the protein fiber composites. Moreover, the kinetic parameters as well as the structural changes of SHMMA and changes of the crystalline and amorphous percentage after grafting with MMA−Ce^{IV} were studied in relation to the weight gain and X-ray diffraction curves. Thus, the successful preparation of Silk fibroin with MMA monomer by graft co-polymerization techniques provides a promising opportunity to widen the potential application of silk composite in biomaterials as well as textile fields.

Materials and Methods

Chemicals and Reagents. *A. assama* protein fiber was collected from a private farm near Jorhat, Assam, India. Because the silk fibroin was processed ready for weaving, no further purification was rendered. MMA was first washed with 5% NaOH solution and then dried with anhydrous sodium sulfate and distilled under nitrogen in reduced pressure.[13] Ceric ammonium sulfate (E-Merck), silica gel (CDH), H_2SO_4 (AR, BDH), and acetone (CDH) were used for this study. Distilled water was used to prepare all solutions.

Preparation of Graft Co-polymerization. The polymerization reactions were carried out in air as the use of nitrogen atmosphere during the time of reaction was found to have no

* To whom correspondence should be addressed. E-mail: amd_das2001@yahoo.co.in.

10.1021/ie100867g
Published on Web 12/20/2010

significant contribution on conversions to graft products.[14] The reaction was set up in a three-necked 300 mL round-bottom flask fitted with stirrer in a temperature controlled water bath. A 1 g amount of dry silk fiber/fabric was swollen with water for 15 min, and it was transferred to the reaction flask containing solutions of ceric ammonium sulfate, H_2SO_4 of different concentrations and the required amount of monomer (MMA) at the required temperature. The reaction time was varied from 1 to 5 h and the temperature of reaction from 35 to 65 °C at a material to liquor ratio of 1:150. The reaction system was intermittently stirred. After the desired reaction time, silks were taken out and were then subjected to repeated extraction with boiling water and acetone to remove homopolymer and its oligomers adhering to the silks. Finally, the products were dried to constant weight and kept in desiccators over P_2O_5.

Conditions Affecting Grafting. Grafting onto silk is a heterogeneous reaction, so the physical structure and the state of aggregation of the silk fiber play an important role. Whatever may be the type of reaction involved in the grafting, chemical bonding is achieved and the synthetic polymer is associated with the protein fiber. In the complex system of protein fiber, monomer, initiator, and acid, several reactions take place simultaneously and the extent of grafting depends on the influence of the chemical conditions, the physical conditions, and the nature of the substrate[15,16] such as (a) diffusion of the monomer to the silk, (b) adsorption of the monomer on the silk, (c) initiation of the active sites on the silk side chain and backbone, (d) formation and propagation of graft on the silk, (e) termination of the active sites on the silk side chain and backbone, (f) homopolymer formation, (g) swelling of the silk, and (h) accessibility of the silk. In the time of graft copolymerization in an aqueous medium, particularly it would be expected to affect the pore size of the silk, the crystalline−amorphous ratio, and the degree of orientation.[17]

Characterization

Thermal Analysis of Copolymers. Thermogravimetric analysis (TGA), differential thermogravimetric (DTG), and differential thermal analysis (DTA) were carried out using a Shimadzu (Model 30) thermal analyzer. The masses of the samples were in the range of 3.95−5.78 mg. α-Alumina was used as a reference material, and the temperature ranged from 30 to 800 °C at heating rates of 10, 20, and 30 °C min^{-1} in a static air atmosphere. Differential scanning calorimetry (DSC) was obtained from a Perkin-Elmer DSC-7 with kinetic software. It consists of a compact central unit and family of cells for DSC thermogravimetry and thermochemical analysis. The heart of the system, the TA processor, functions as a combination of control unit, computer power unit, and interface to be used through the keyboard and display. The DSC 20 standard cell is used for heat flow measurement in the temperature range ambient to 800 °C.

Kinetic Parameters. The kinetics of polymer degradation is usually represented by the basic kinetic[18]

$$d\alpha/dt = k(T)\, f(\alpha) \tag{1}$$

where α represents the conversion (extent of reaction; α = 0−1), t is the time, $k(T)$ is the rate constant, and $f(\alpha)$ is the reaction model, which describes the dependence of the reaction rate on the extent of reaction. The temperature dependence of $k(T)$ could be represented by the Arrhenius equation

$$d\alpha/dt = Ae^{-E_a/RT} f(\alpha) \tag{2}$$

where E_a is the activation energy of the process. A is the preexponential factor, R is the universal gas constant, and $f(\alpha)$ depends on the decomposition mechanism. The simplest and most frequently used model for $f(\alpha)$ is

$$f(\alpha) = (1 - \alpha)^n \tag{3}$$

where n is the order of reaction.

The rate of conversion, $d\alpha/dt$, at constant temperature can be expressed by

$$d\alpha/dt = k = k(T)\, f(\alpha) \tag{4}$$

and finally combining eqs 2−4 gives the following relationship

$$d\alpha/dt = k = (1 - \alpha)^n A e^{-E_a/RT} \tag{5}$$

and eq 5 can be expressed for first-order reaction by the following relationship

$$d\alpha/dt = k = Ae^{-E_a/RT} \tag{6}$$

In short, the Arrhenius equation is an expression that shows the dependence of the rate constant k of chemical reactions on the temperature T and activation energy E_a, as shown above. In chemical kinetics a reaction rate constant quantifies the speed of a chemical reaction. In chemical kinetics, the frequency factor or A factor is the preexponential constant in the Arrhenius equation, which indicates how many collisions between reactants have the correct orientation to lead to the products. The logarithm of the Arrhenius equation is represented by the following

$$\ln(k) = -E_a/RT + \ln(A) \tag{7}$$

So, when a reaction has a rate constant which obeys the Arrhenius equation, a plot of $\ln(k)$ versus T^{-1} gives a straight line, whose slope and intercept can be used to determine E_a and A. That is, the activation energy is defined to be $-R$ times the slope of a plot of $\ln(k)$ vs $(1/T)$.

$$E_a = -R(\delta(\ln k)/\delta(1/T)) \tag{8}$$

The Arrhenius equation gives the quantitative basis of the relationship between the activation energy and the rate at which a reaction proceeds.

Coats and Redfern Method. The retrieval of kinetic parameters from weight loss versus temperature data could be carried out by using various methods.[19,20] In the present work, the well-known Coats and Redfern method was used for retrieving kinetic parameters from dynamic thermogravimetry. The general correlation equation used in the Coats and Redfern method is

$$\log[1 - (1 - \alpha)^{1-n}/T^2(1 - n)] = \log[AR/\alpha E_a(1 - 2RT/E_a)] - E/2.3RT \tag{9}$$

where α is the reaction decomposed at temperature T, n is the order of the reaction, A is the frequency factor (S^{-1}), a is the heating rate (K min^{-1}), R is the gas constant (kJ mol^{-1} K^{-1}), T

Scheme 1

$$(NH_4)_4Ce(SO_4)_4 \rightleftharpoons Ce(SO_4)_4^{2-} + 4\,(NH_4)^+$$

$$Ce(SO_4)_4^{2-} \rightleftharpoons Ce^{4+} + 4\,SO_4^{2-}$$

Scheme 2. Free Radical Reaction Mechanism of the Graft Co-polymerization Reaction System[a]

Step I : Initiation

Ce^{IV} system :

$$Ce^{4+} + SH \overset{K_1}{\rightleftharpoons} \text{Complex 1} \xrightarrow{Kr_1} \dot{S} + Ce^{3+} + H^+ \quad (1)$$

$$\dot{S} + M \xrightarrow{k_i} \dot{SM} \quad \text{(Initiation of grafting)} \quad (2)$$

$$M + Ce^{4+} \overset{K_2}{\rightleftharpoons} \text{Complex 2} \xrightarrow{Kr_2} \dot{M} + Ce^{3+} + H^+ \quad (3)$$

(Initiation of homopolymerization)

$$\dot{SM} + H_2O \longrightarrow SMH + \dot{O}H$$

$$\dot{O}H + M \longrightarrow OH - M$$

Step II : Propagation

$$\dot{SM} + M \xrightarrow{k_p} \dot{SM}_2$$
$$\dot{SM}_{n-1} + M \xrightarrow{k_p} \dot{SM}_n$$

Propagation of grafting

$$\dot{M} + M \longrightarrow \dot{M}_2$$
$$\dot{M}M_{n-1} + M \longrightarrow \dot{M}_n$$

Propagation of homopolymerization

Step III : Oxidation

Ce^{IV} system :

$$\dot{SM}_n + Ce^{4+} \xrightarrow{k_t} SM_n + Ce^{3+} + H^+ \quad \text{(Termination of grafting)}$$

$$\dot{M}_n + Ce^{4+} \longrightarrow M_n + Ce^{3+} + H^+$$

$$\dot{S} + Ce^{4+} \xrightarrow{k_o} \text{Oxidized product} + Ce^{3+} + H^+$$

Now,

$$\frac{d[\dot{SM}n]}{dt} = [\dot{S}][M] - [\dot{SM}n][Ce^{4+}]k_t = 0$$

$$[\dot{SM}n] = \frac{k_i[\dot{S}][M]}{[Ce^{4+}]k_t}$$

$$\frac{d[\dot{S}]}{dt} = k_d[SH][R^{\cdot}] - k_i[\dot{S}][M] - k_o[\dot{S}][Ce^{4+}] = 0$$

$$[S^{\cdot}] = \frac{k_d[SH][R^{\cdot}]}{k_i[M] - k_o[Ce^{4+}]}$$

$$R_p = k_p[\dot{SM}n][M] = \frac{k_p k_d k_i [SH][M]^2}{k_t[M\,n^{4+}][k_i[M] + k_o[M\,n^{4+}]}$$

$$= \frac{k_p k_i}{k_t} \cdot \frac{k_p k_d k_i [SH][M]^2}{[M\,n^{4+}][k_i[M] + k_o[M\,n^{4+}]}$$

[a] Where SH, SMn$^{\bullet}$, M, and Mn$^{\bullet}$ represent the silk molecule, silk monomer macroradical, monomer, and monomer macroradicals, respectively.

is the temperature (K), and E is the activation energy (kJ mol^{-1}). A computer program in FORTRAN 77 was used for the linear least-squares analysis with Gauss−Jordan subroutine and applied to evaluate n, ΔE, A, and SED simultaneously. The procedure

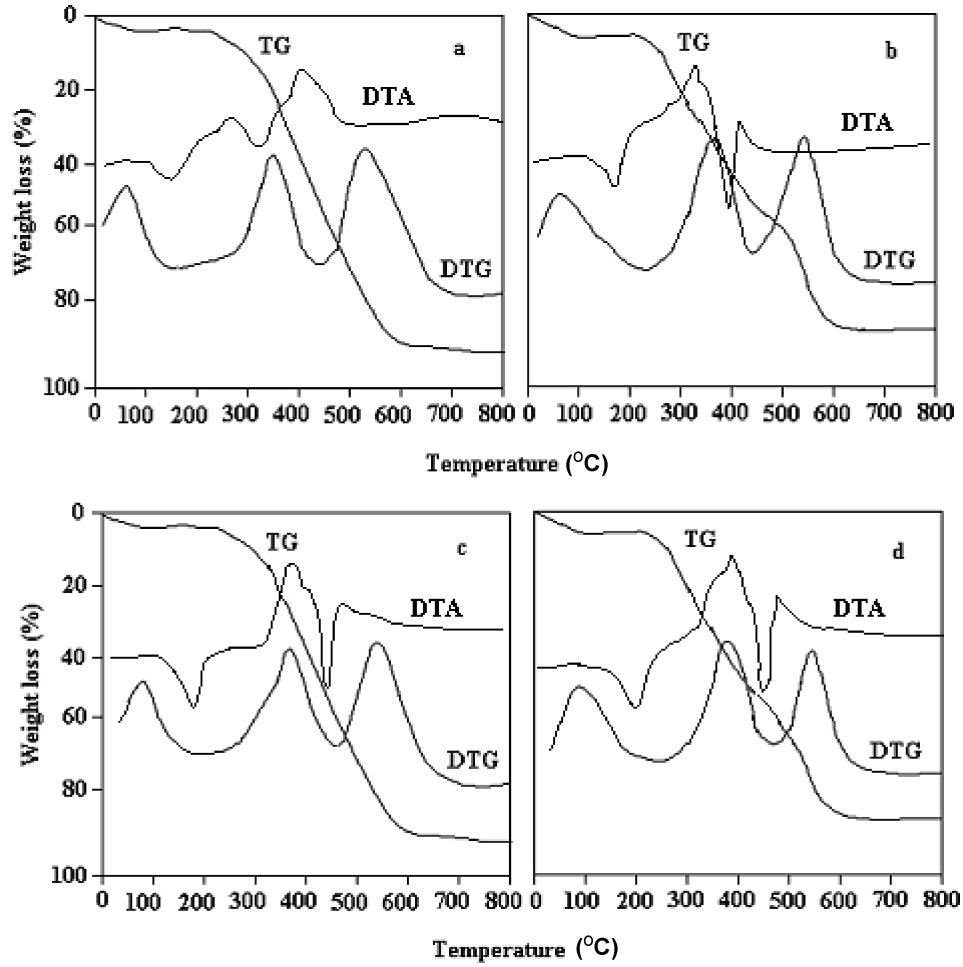

Figure 1. Thermogravimetric analysis (TGA), differential thermogravimetry (DTG), and differential thermal analysis (DTA) curves at a heating rate of 20 °C/min: (a) ungrafted, (b) 49% SHMMA, (c) 59% SHMMA, and (d) 71% SHMMA.

Table 1. (a) Thermal Analysis Data (Active Decomposition Temperature and Weight Loss for Ungrafted and SHMMA at Heating Rates of 20 °C/min) and (b) DTA Data (Decomposition Temperature)[a]

		at 20 °C/min								
		(a) thermal analysis data						(b) DTA data		
		weight loss,[b] %			active decomposition temp, °C			decomposition temp, °C		
samples	%	I	II	III	I	II	III	I	II	−
ungrafted	−	12.5 (30−140)	41.8 (150−390)	43.0 (390−640)	60 (endo)	360 (endo)	520 (endo)	150 (endo)	350 (endo)	−
grafted	49	10.2 (30−170)	38.0 (175−430)	45.5 (440−675)	80 (endo)	380 (endo)	550 (endo)	175 (endo)	395 (endo)	365 (exo)
	59	8.9 (30−180)	36.8 (185−450)	48.8 (455−695)	90 (endo)	390 (endo)	565 (endo)	182 (endo)	420 (endo)	380 (exo)
	71	7.2 (30−190)	33.0 (195−470)	47.5 (480−720)	95 (endo)	400 (endo)	585 (endo)	200 (endo)	435 (endo)	405 (exo)

[a] I, II, and III are the prestage, second stage, and third stage, respectively. [b] Temperature range (°C) in parentheses.

Table 2. (a) Thermal Analysis Data (Active Decomposition Temperature and Weight Loss for Ungrafted and SHMMA at Heating Rates at 30 °C/min) and (b) DTA Date (Decomposition Temperature)[a]

		at 30 °C/min								
		(a) thermal analysis data						(b) DTA Data		
		weight loss,[b] %			active decomposition temp			decomposition temp		
samples	%	I	II	III	I	II	III	I	II	−
ungrafted	−	13.8 (30−160)	48.0 (170−400)	32.0 (400−700)	70 (endo)	365 (endo)	540 (endo)	160 (endo)	355 (endo)	−
grafted	49	11.8 (30−175)	46.5 (180−420)	35.8 (430−720)	80 (endo)	385 (endo)	570 (endo)	190 (endo)	415 (endo)	380 (exo)
	59	9.6 (30−190)	43.9 (195−440)	39.7 (445−740)	90 (endo)	390 (endo)	585 (endo)	200 (endo)	430 (endo)	405 (exo)
	71	8.5 (30−195)	41.8 (205−455)	37.0 (460−760)	95 (endo)	410 (endo)	605 (endo)	210 (endo)	455 (endo)	420 (exo)

[a] I, II, and III are prestage, second stage, and third stage. [b] Temperature range (°C) in parentheses.

basically involved stepwise change of n (over a range of 0.6−1.6) to determine the SED in the least-squares estimate of the parameters ΔE and A. The data were found to fit well for a first-order reaction.

XRD of Co-polymers. X-ray diffraction data were collected using a computer-controlled X-ray diffractometer (Type, JDX-11P3A, JEOL) with pulse-height analyzer and scintillation counter. Measuring conditions were as follows: mode, step; KV,

Table 3. Experimental Conditions and Kinetic Data of the Coats and Redfern Equation

samples % grafted	temp, °C	I (first stage) E, kJ mol^{-1}	I (first stage) A, S^{-1}	I (first stage) SED, S^{-1}	II (second stage) E, kJ mol^{-1}	II (second stage) A, S^{-1}	II (second stage) SED, S^{-1}
49	20	33.781	0.398	0.001	38.582	0.672	0.002
	30	36.123	0.643	0.001	41.321	0.997	0.001
	40	38.921	1.023	0.002	42.561	1.462	0.003
	50	41.746	1.721	0.001	44.626	2.103	0.002
59	20	37.250	0.7601	0.002	42.821	0.908	0.002
	30	39.524	1.502	0.001	46.309	1.752	0.001
	40	42.881	2.598	0.003	48.147	2.962	0.003
	50	48.978	4.833	0.004	51.001	5.125	0.002
71	20	44.216	0.938	0.003	49.779	6.998	0.004
	30	45.998	2.431	0.001	54.512	9.985	0.001
	40	47.102	4.381	0.004	57.124	14.851	0.003
	50	56.892	8.462	0.002	61.324	20.861	0.001

Table 4. Logarithmic Data Using the Arrhenius Equation at Different Stages (From the Coats and Redfern Equation)

samples % grafted	temp, K	I (first stage) $1/T$	I (first stage) ln k	I (first stage) R^2	II (second stage) $1/T$	II (second stage) ln k	II (second stage) R^2
49	293	0.0034	−0.934	0.9994	293	−0.413	0.9997
	303	0.0033	−0.455	−	303	−0.019	−
	313	0.0032	0.008	−	313	0.364	−
	323	0.0031	0.527	−	323	0.726	−
59	293	0.0034	−0.259	0.999	293	−0.114	0.9982
	303	0.0033	0.391	−	303	0.542	−
	313	0.0032	0.938	−	313	1.067	−
	323	0.0031	1.557	−	323	1.615	−
71	293	0.0034	−0.082	0.9982	293	1.925	0.9992
	303	0.0033	0.711	−	303	2.279	−
	313	0.0032	1.459	−	313	2.676	−
	323	0.0031	2.114	−	323	3.015	−

40; start angle, 2°; target, Cu; mA, 20; stop angle, 60°; measuring time, 0.5 s; step angle, 0.05. The degree of crystallinity (K_c) was found using the following equation.[21]

$$K_c = \int_0^{\alpha} S^2 I_c(S)\, dS / \int_0^{\alpha} S^2 I(S)\, dS \qquad (10)$$

where S is the magnitude of the reciprocal lattice vector and S is given by

$$S = 2 \sin \theta / \lambda$$

where θ is half of the angle of deviation of the diffracted rays from the incident X-rays, λ is the X-ray wavelength, $I(S)$ is the intensity of coherent X-ray scatter from a specimen (both crystalline and amorphous), and $I_c(S)$ is the intensity of coherent X-ray scatter from the crystalline region.

Result and Discussion

Possible Mechanism for Graft Co-polymerization. Grafting of vinyl monomers to SH is a typical free radical polymerization reaction, which involves three distinct aspects, such as initiation, propagation, and termination. The formation of free radicals on the SH molecule can occur by the homolytic cleavage processes, such as dehydrogenation, dehydroxylation, and depolymerization. The location of the free radicals sites on the SH molecule and within the fibrous structure is dependent on the method of initiation of such sites and on the physical and chemical properties of the SH.[22]

The precise reaction and mechanism governing the grafting of vinyl monomers onto SH are difficult to determine since the reaction is heterogeneous. The ceric ion initiation of grafting has gained considerable importance because this method can be applied for initiating grafting of synthetic monomers to a number of macromolecules.

When SH is oxidized by Ce^{IV} salt, ceric ammonium sulfate, free radicals capable of initiating vinyl polymerization are formed exclusively on the SH side chain and backbone by a single free electron transfer.[23]

Ceric ammonium sulfate exists as a complex salt and is ionized in solution, yielding free ammonium ions and sulfatocerate ions. The sulfatocerate ions subsequently decomposed to yield Ce^{IV} cations and sulfate anions[15] (Scheme 1).

The reactions during graft co-polymerization of MMA onto SH with the Ce^{IV} system in the presence of H_2SO_4 may take place as shown in Scheme 2.

The free radical ($R^{\bullet}$) formed in the graft co-polymerization process might attack the SH molecule, giving rise to SH macroradicals ($S^{\bullet}$) in the following manner.[24]

$$SH + R^{\bullet} \xrightarrow{k_d} S^{\bullet} + RH$$

Thermal Analysis. The thermal behavior of ungrafted and grafted products was studied from TG, DTG, and DTA at heating rates of 20 and 30 °C/min, and different percentage of grafting for a heating rate of 20 °C/min are shown in Figure 1. The decomposition temperature ranges, the active decomposition temperatures, and the percent weight losses are given in Table 1a,b and Table 2a,b.

The decomposition took place in three distinct stages referred to as initiation, propagation, and carbonization,[25,26] and all of the TG curves showed an initial small mass loss step around 150 °C, which could be attributed to the removal of absorbed water. In the second stage, a major weight loss was noticed at a heating rate of 20 °C/min for ungrafted and grafted products. The decomposition of protein started at 150 °C for ungrafted product, which increased for 49% grafted at 175 °C, 59% grafted at 185 °C, and 71% grafted at 195 °C, depending on the increasing percent of grafting, while, in the third stage, decomposition of the rest of the polymers started at 390 °C for ungrafted and increased for 49% grafted at 440 °C, 59% grafted at 455 °C, and 71% grafted at 480 °C (Table 1a), respectively.

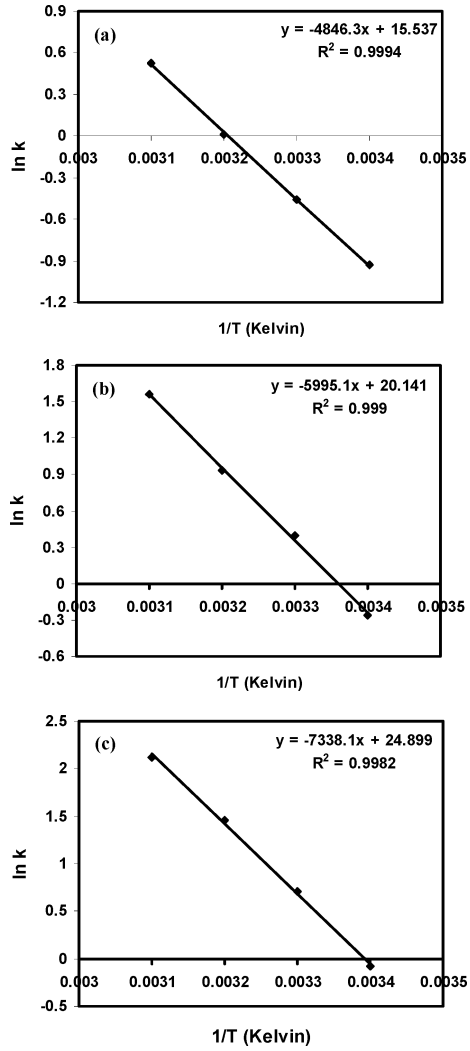

Figure 2. Plots of ln k vs $1/T$ of the first-stage thermal decomposition of SHMMA using Arrhenius equation data from the Coats and Redfern equation: (a) 49, (b) 59, and (c) 71%.

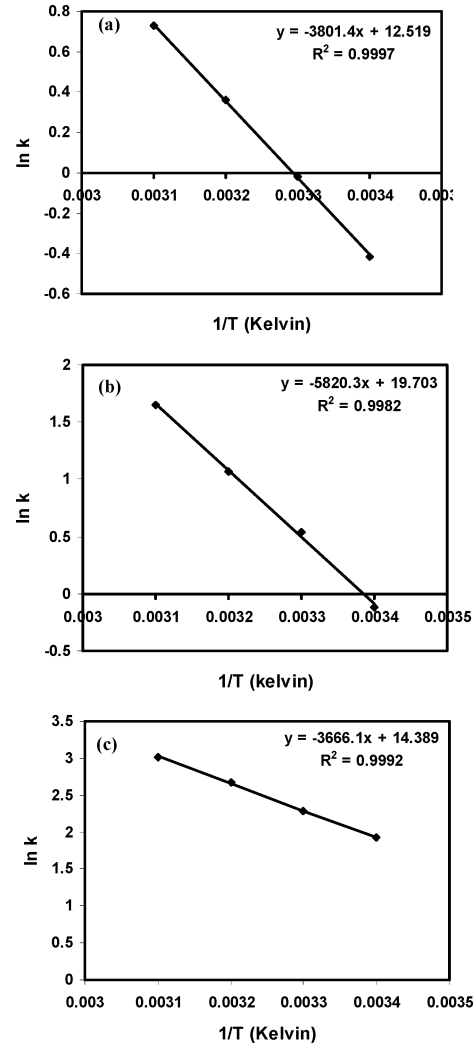

Figure 3. Plots of ln k vs $1/T$ of the second-stage thermal decomposition of SHMMA using Arrhenius equation data from the Coats and Redfern equation: (a) 49, (b) 59, and (c) 71%.

The weight loss percent of the grafted fiber was found to be less than that of the ungrafted fiber, as evident from Tables 1a and 2a, which show the initial, maximum, and final temperatures of active decomposition increased with an increase in the grafting percent of SHMMA. A similar trend was also observed at a heating rate of 30 °C/min.

The DTA curves at the heating rate 20 °C/min showed an endothermic peak at 150 °C for ungrafted SH, and the same appeared at in increasing order for grafted composites, i.e., 175, 182, and 200 °C for 49, 59, and 71% grafted SH, respectively. Similarly, the second endothermic peak appeared at 350 °C for ungrafted SH, and the same shifted to in increasing order for grafted composites, i.e., 395, 420, and 435 °C for 49, 59, and 71% grafted SH, respectively. Exothermic peaks also appeared for grafted composites at 350, 380, and 405 °C for 49, 59, and 71% grafted SH due to a change in crystallinity.[27]

Kinetics Studies. For studying the kinetics of SHMMA composites, we applied the Coats and Redfern method using computer program FORTRAN 77 for linear least-squares method with Gauss−Jordan subroutine. The values of activation energy, frequency factors, and error deviation are shown in Table 3 in four different temperatures, 20, 30, 40, and 50 °C, for SHMMA composites of 49, 59, and 71%. The values were found to be higher than that of the ungrafted original one. These values increased with an increase in the molecular weights. We have also applied the Arrhenius equation for first-order reaction, which is fit well in our reaction process, and plotted graphs ln k versus $1/T$ for each reaction temperature of the first and second stages of the thermal decompositions, which are shown in Table

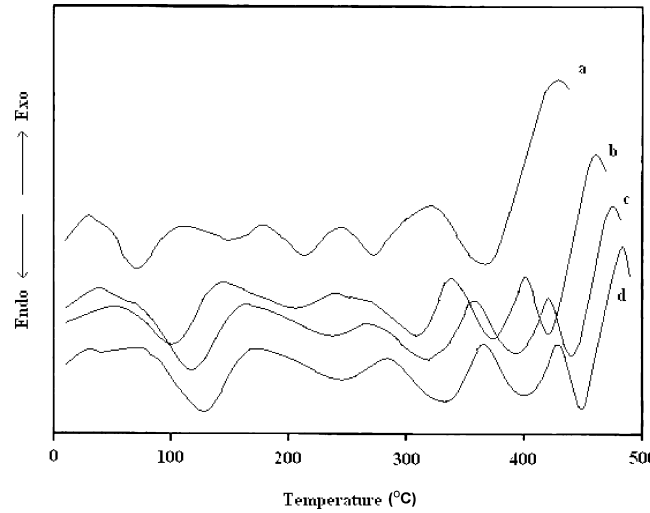

Figure 4. Differential scanning calorimetry curves for the decomposition of (a) ungrafted and (b) 49, (c) 59, and (d) 71% SHMMA composite.

Table 5. (a) Thermal Analysis Data for Decomposition Temperature and Glass Transition (T_g) Values of Ungrafted and SHMMA at a Heating Rate of 20 °C/min and (b) X-ray Diffraction Data and Crystallinity of Ungrafted and SHMMA

(a) thermal analysis data				(b) X-ray diffraction data and crystallinity		
samples	%	decomposition temp (°C)	T_g (°C)	X-ray diffraction data (d′ spacing in A^0)	2θ	crystallinity (%)
ungrafted	–	92	175	6.772 (100)	9.03	33
	–	234	175	*4.553 (72)*	18.40	33
	–	297	175	*3.825 (65)*	20.02	33
	–	370	175	--	--	–
grafted	49	107	225	7.927 (100)	12.05	46
	49	327	225	*5.726 (87)*	18.36	46
	49	390	225	*4.821(81)*	22.51	46
	49	435	225	–	–	–
	59	120	260	*8.234 (100)*	13.54	54
	59	335	260	*7.231 (89)*	19.32	54
	59	400	260	*5.822 (83)*	22.65	54
	59	450	260	–	–	–
	71	131	275	10.021 (100)	13.78	62
	71	347	275	*8.019 (93)*	22.98	62
	71	415	275	6.246 (77)	27.32	62
	71	465	275	–	–	–

4 and Figures 2a−c and 3a−c, and confirmed that the degradation of the polymer composites was indeed first order. The correlation coefficients R were calculated from the graphs and are shown in the figures. The values were found to be higher than that of the ungrafted original one and increased with an increase in the molecular weights in both of the degradation stages. The value of the correlation coefficients R was also calculated from the slope and intercept of the straight lines, and it was observed that the change of the activation energy was significant in the grafted polymer composites. Contrarily, the decomposition temperature and activation energy of the grafted samples were found to be at higher temperature, suggesting that the high temperature provided favorable conditions to form more stable structures during the grafting. The treatment also increased the crystallinity index of the fibers, resulting in a higher degradation temperature.

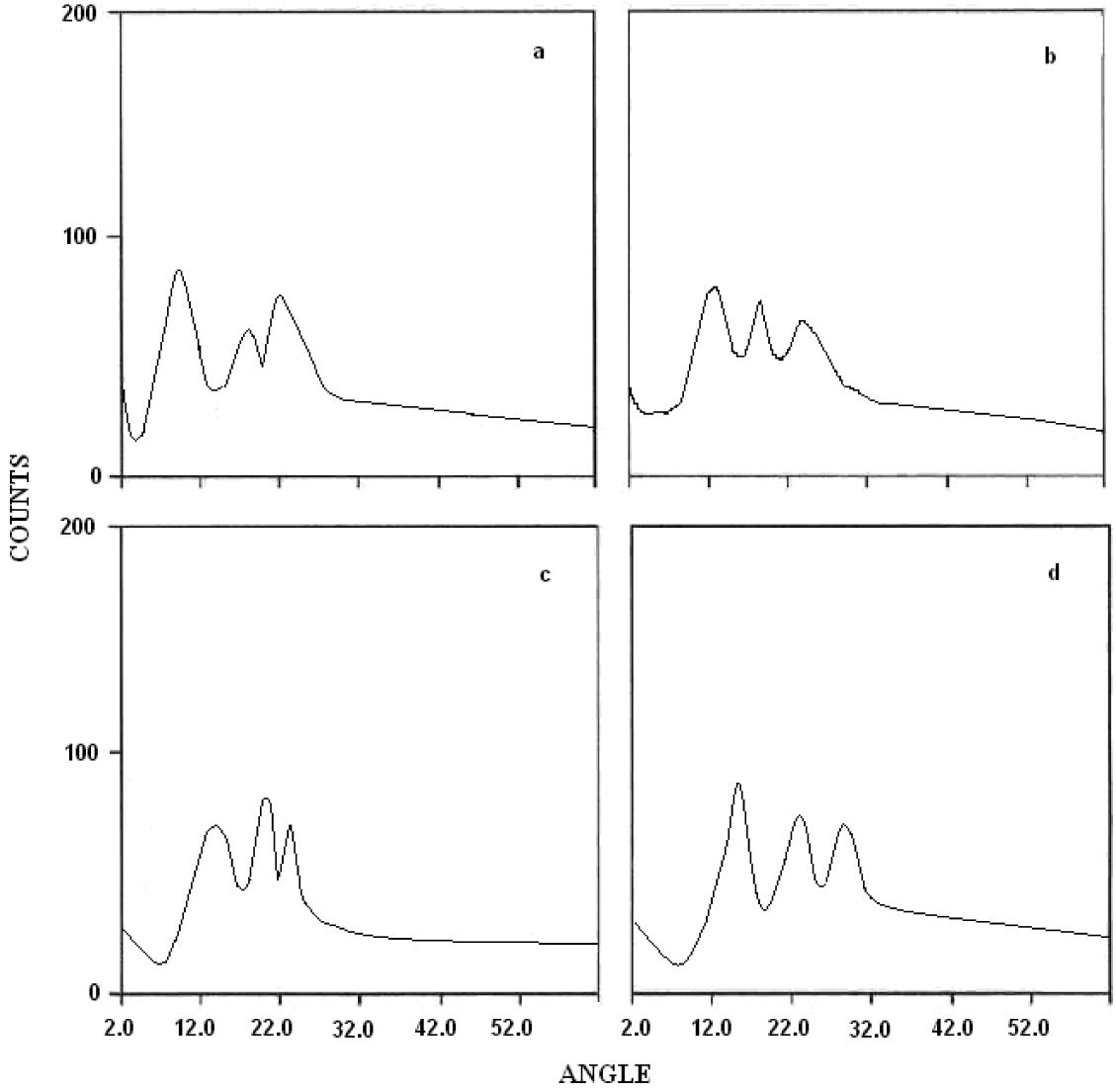

Figure 5. XRD patterns of the (a) ungrafted and (b) 49, (c) 59, and (d) 71% SHMMA composite.

Scheme 3. Schematic Representation of the Structural Changes During Graft Co-polymerization of SH[a]

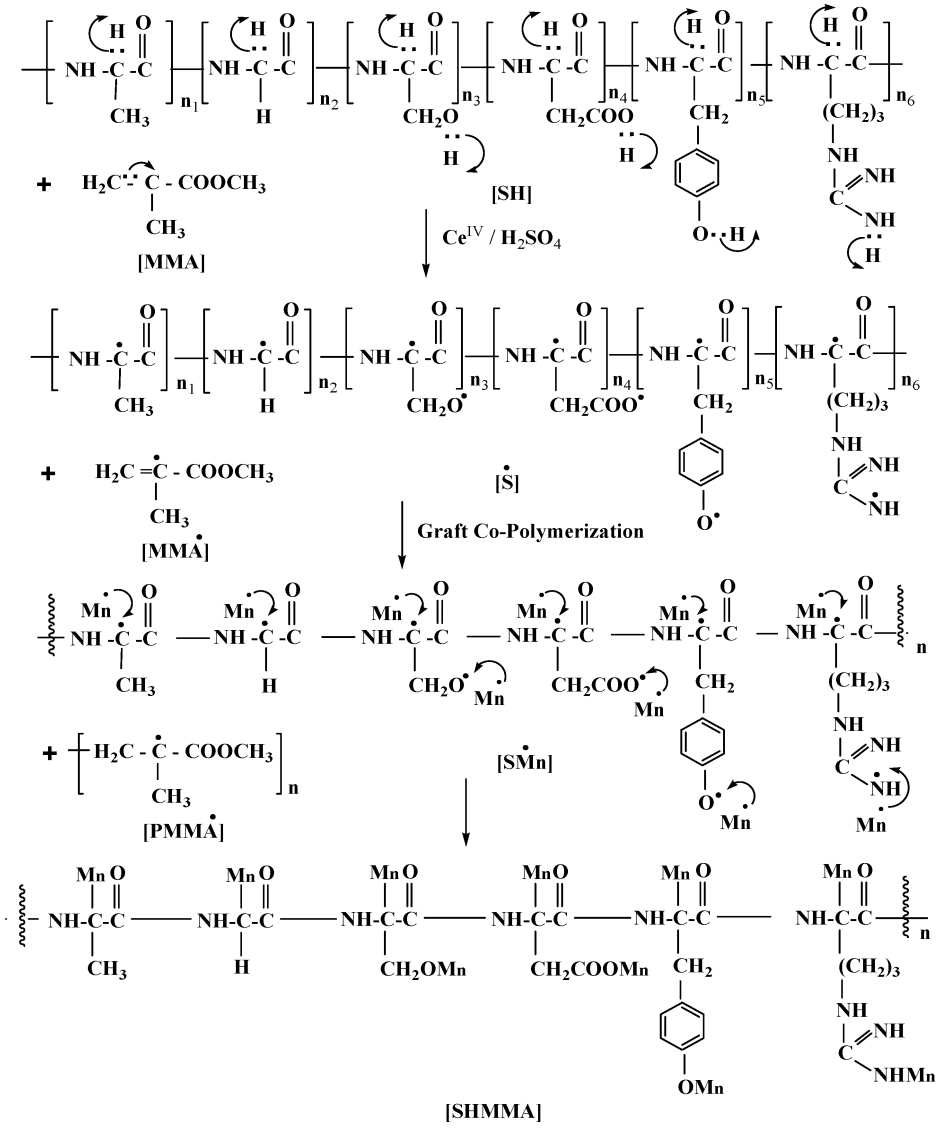

[a] Where SH is the silk molecule, S• is the silk-free radical, and Mn represents poly(methyl methacrylate) (PMMA).

Table 6. Grafting on *Antheraea assama* Silk Composites by the MMA−Ce^{IV} System with (a) Variation of Reaction Time and Temperature and (b) Variation of Monomer Concentration[a]

(a)		(b)								
		at given temp				at given monomer concn *M*				
grafting param	time of reacn, h	35 °C	45 °C	55 °C	65 °C	50 mol/L	60 mol/L	70 mol/L	80 mol/L	90 mol/L
graft yield (%)	1	18	23	33	28	33	40	47	54	49
	2	24	29	39	35	39	46	52	60	56
	3	30	36	47	45	47	58	63	75	67
	4	37	45	58	52	58	65	71	88	78
	5	31	39	51	48	51	60	66	77	71
total conversion (%)	1	8.8	10.0	12.4	11.3	12.5	15.9	18.2	19.6	18.9
	2	11.5	12.1	15.1	14.1	15.1	18.7	21.0	24.2	22.0
	3	13.8	14.6	17.8	16.8	17.8	24.1	26.5	29.6	27.2
	4	15.0	17.2	20.1	18.7	20.1	26.0	29.3	33.3	31.0
	5	13.7	15.3	17.9	17.4	17.9	25.3	27.7	31.0	28.6
grafting efficiency (%)	1	30.0	33.8	37.9	36.4	37.9	39.6	41.2	43.3	42.0
	2	30.8	35.4	38.8	35.6	38.8	41.5	43.0	44.5	43.9
	3	33.3	36.6	39.3	37.5	39.3	42.4	44.5	46.0	45.2
	4	36.3	38.5	42.6	40.9	42.6	44.8	46.6	48.2	47.0
	5	33.9	37.4	41.8	38.2	41.8	43.0	45.1	46.7	45.9
rate of grafting × 10^6	1	3.3	4.3	6.1	5.2	6.1	7.3	8.7	9.9	9.1
	2	2.2	2.7	3.6	3.2	3.6	4.3	4.8	5.5	5.2
	3	1.8	2.2	2.9	2.8	2.9	3.6	3.9	4.6	4.1
	4	1.7	2.1	2.7	2.4	2.7	3.0	3.3	4.1	3.6
	5	1.1	1.4	1.9	1.8	1.9	2.2	2.4	2.8	2.6

[a] The results are averages of three readings. Conditions: Silk composites, 1 g; ceric ammonium sulfate, 15×10^{-3} M; H_2SO_4 acid, 15×10^{-2} M; material to liquor ratio, 1:150 (M = molar); with (a) MMA of 50×10^{-2} M and (b) temperature of 50 °C.

Scheme 4. Diagrammatic Representation of the Grafted Silk Molecule

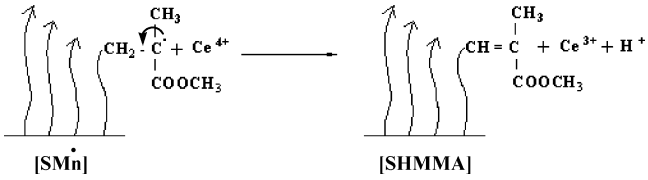

Differential Scanning Calorometry Properties. The thermal behavior of ungrafted and SHMMA composites of different grafting percent were studied with the help of DSC[8,28], at a heating rate of 20 °C/min, and the thermograms and data have been presented in Figure 4 and Table 5a. In the case of the ungrafted one, the first broad endotherm below 100 °C is due to the evaporation of water. Two minor and broad endothermic transitions appeared at 234 and 297 °C (shoulder form), followed by a prominent endothermic peak at 370 °C.

In the case of SHMMA, the endothermic peak due to evaporation of water shifted to higher temperature as the grafting increased. However, the SHMMA showed an endothermic peak at 107, 120, and 131 °C for 49, 59, and 71% grafted products, respectively. The minor peaks (shoulder form) were shifted to 327, 335, and 347 °C for the SH due to enthalpic change and another endothermic peak was observed in each of the grafted SH at 390, 400, and 415 °C for 49, 59, and 71% grafted SH. On the basis of the above DSC results, it was assumed that the endothermic peaks at 435, 450, and 465 °C for the SH were related to the presence of the MMA polymer in the SH molecule. The glass transition temperatures (T_g) for the grafted SH were found to be 225, 260, and 275 °C for 49, 59, and 71% SHMMA composites and have been shown in Table 5a.

X-ray Diffraction Studies. The XRD patterns of SH grafted with MMA have been shown in Figure 5, and the data obtained have been tabulated in Table 5b. The XRD patterns exhibited the presence of both amorphous and crystalline regions.[29,30] However, the crystalline regions were more prominent in the case of grafted products, in comparison to the original ungrafted SH composites. From the data, it was evident the crystallinity percentages in SHMMA composites were found to be more than that of ungrafted one. The increase in crystallinity character in SHMMA products indicated that, on grafting, the SH molecule had under gone an isomeric change; in other words, the SH molecule which was atactic had changed to isotactic after grafting with MMA using the Ce^{IV} redox initiator system. Therefore, it might be suggested that the structural rearrangement of SHMMA composites took place during grafting, as given in Scheme 3. In this scheme, the structure of SH, which consisted mainly of the amino acid residues of glycine, alanine, serine aspartic acid, tyrosine, and arginine, has been represented in one dimension, and the strategy was given to describe the way of attacking by the monomer free radical and finally the SHMMA polymer composites. The diagrammatic representation of SHMMA was also given in Scheme 4.

Comparative Study of the Effects of Temperature and Time on Grafting. A comparative study of the effects of reaction temperature on grafting of MMA onto SH fibers/fabrics was carried out at four different temperatures ranging from 35 to 65 °C. It was evident from Table 6a that the weight gain increased steadily up to 55 °C, and beyond that the rate gradually slowed, which could be ascribed due to the greater activation energy. As the temperature of the reaction increased, the swellability of the SHMMA is greatly enhanced and as such the diffusion of the monomer from the solution phase to the SH phase took place.[31] The study also was carried out on reaction time for 1−5 h duration. The graft yield percentage increased with the increase in the time of reaction up to 4 h, and after that the rate of grafting slowed (Table 6a). It can be concluded that is due to depletion in the available active centers on the substrate backbone as the reaction proceeded.[32]

Studies on Variation of Monomer Concentrations. The variation of the phenomenon incorporated in the graft copolymerization reactions was carried out using five different concentrations of the monomer MMA (methyl methacrylate) from 50×10^{-2} to 90×10^{-2} M (mol/L). The remaining reaction conditions were kept constant. With the increase in monomer concentrations up to 80×10^{-2} M, the rate of grafting increased gradually and decreased thereafter and has been shown in Table 6b. It can be described that, at a certain monomer concentration, combination of monomer probably took place with SH composites. The concentration of $PMMA^{\bullet}$ increased with the rate of their combination faster than the rate of their combination with SH composites.[33]

Conclusions

In this study, a strategy is described for a potential new technique for thermostable biodegradable composites using MMA and Ce^{IV}, and it has gotten good results from the reaction systems. The grafting percentage of the reaction system was dependent on temperature, time, and monomer concentrations, which have been evident from the data. From thermal analysis data and kinetic parameters, it was observed that grafted SHMMA was found to be thermally more stable than the SH composites and followed first-order Arrhenius rate equation. The MMA and Ce^{IV} system does not lead to deleterious effects on the color and other chemical properties of the protein fiber. Besides this, this would be of great importance for further modification of the SH, which have great potential to be constructed into biomaterials as well as the best textiles.

Acknowledgment

We thank the Director, Dr. P. G. Rao, North East Institute of Science & Technology (CSIR), Jorhat, India, for his kind permission to publish this paper.

Literature Cited

(1) Sing, V.; Tiwari, A.; Pandey, S.; Sing, S. K. Peroxy-disulphate initiated synthesis of potato starch-graft PAN under microwave irradiation. *eXPRESS Polym. Lett.* **2007**, *1*, 51.

(2) Hazarika, L. K.; Saikia, C. N.; Kataky, A.; Bordoloi, S.; Hazarika, J. Evaluation of physico-chemical characteristics of silk fibres of *Antheraea assama* reared on different host plants. *Bioresour. Technol.* **1998**, *64*, 67.

(3) Asakura, T.; Sugino, R.; Yao, J. M.; Takashima, H.; Kishore, R. Comparative structure analysis of tyrosine and valine residues in unprocessed silk fibroin (silk I) and in the processed silk fiber (silk II) for *Bombyx mori* using solid-state ^{13}C, ^{15}N, and ^{2}H NMR. *Biochemistry* **2002**, *41*, 4415.

(4) Jin, H.-J.; Park, J.; Valluzzi, R.; Cebe, P.; Kaplan, D. L. Biomaterial films of *Bombyx mori* silk fibroin with poly(ethylene oxide). *Biomacromolecules* **2004**, *5*, 711.

(5) Zhang, K.; Wang, H.; Huang, C.; Su, Y.; Mo, X.; Ikada, Y. Fabrication of silk fibroin blended P(LLA-CL) nanofibrous scaffolds for tissue engineering. *J. Biomed. Mater. Res.* **2009**, *43*, 114.

(6) Marsanoa, E.; Corsinia, P.; Canettib, M.; Freddic, G. Regenerated cellulose-silk fibroin blends fibers. *Int. J. Biol. Macromol.* **2008**, *43*, 106.

(7) She, Z.; Liu, W.; Feng, Q. Preparation and cytocompatibility of silk fibroin/chitosan scaffolds. *Front. Mater. Sci. China* **2009**, *3*, 241.

(8) Cheung, H.-Y.; Lau, K.-T.; Tao, X.-M.; Hui, D. A potential material for tissue engineering: Silkworm silk/PLA biocomposite. *Composites, Part B* **2008**, *39*, 1026.

(9) Tang, Y.; Cao, C.; Ma, X.; Chen, C.; Zhu, H. Study on the preparation of collagen-modified silk fibroin films and their properties. *Biomed. Mater.* **2006**, *1*, 242.

(10) Jin, H.-J.; Park, J.; Valluzzi, R.; Cebe, P.; Kaplan, D. L. Structure and properties of silk hydrogels. *Biomacromolecules* **2004**, *5*, 711.

(11) Hoefnagels, H. F.; Wu, D.; de With, G.; Ming, W. Biomimetic superhydrophobic and highly oleophobic cotton textiles. *Langmuir* **2007**, *23*, 13158.

(12) Kessler, M. R.; White, S. R. Cure kinetics of the ring-opening metathesis polymerization of dicyclopentadiene. *J. Polym. Sci., Part A: Polym. Chem.* **2002**, *40*, 2373.

(13) Liu, Y.; Yang, L.; Shi, Z.; Li, J. Graft copolymerization of methyl acrylate onto cellulose initiated by potassium ditelluratoargentate (III). *Polym. Int.* **2004**, *53*, 1561.

(14) Das, A. M.; Chowdhury, P. K.; Saikia, C. N.; Rao, P. G. Some physical properties and structure determination of vinyl monomer-grafted Anthearea assama silk fiber. *Ind. Eng. Chem. Res.* **2009**, *48*, 9338.

(15) Jian, M. J.; Hui, J. Z.; Guang, L.; Jin, J. H.; Sheng, L. Y. Poly (P-phenylene benzoxazole) fibre chemically modified by the incorporation of sulfonate groups. *J. Appl. Polym. Sci.* **2008**, *109*, 3133.

(16) Bhattacharyya, A.; Misra, B. N. Grafting: A versatile mean to modify polymers techniques, factors and applications. *Prog. Polym. Sci.* **2004**, *29*, 767.

(17) Mingzhong, Li.; Norihiko, M.; Lixing, D.; Linsen, Z. Preparation of porous poly(vinyl alcohol)−silk fibroin (PVA/SF) blend membranes. *Macromol. Mater. Eng.* **2001**, *286*, 529.

(18) Wang, J.; Wenhui, W.; Zhihui, L. Kinetics and thermodynamics of the water sorption of 2-hydroxyethyl methacrylate/styrene copolymer hydogels. *J. Appl. Polym. Sci.* **2008**, *109* (5), 3018.

(19) Coats, A. W.; Redfern, J. R. Kinetic parameters from thermogravimetric data. *Nature* **1964**, *68*, 201.

(20) Rabek, J. F. *Experimental methods in polymer chemistry*; John Wiley & Sons: London, 1980.

(21) Jayakumar, R.; Prabaharan, M.; Reis, R. L.; Mano, J. F. Graft copolymerized chitosan-present status and applications. *Carbohydr. Polym.* **2005**, *62*, 142.

(22) Xie, F.; Zhang, H.; Shao, H.; Hu, X. Effect of shearing on formation of silk fibers from regenerated *Bombyx mori* silk fibroin aqueous solution. *Int. J. Biol. Macromol.* **2006**, *38*, 284.

(23) Kaith, B. S.; Kalia, S. Graft copolymerization of MMA onto flax under different reaction conditions: a comparative study. *eXPRESS Polym. Lett.* **2008**, *2*, 93.

(24) Rahman, M. R.; Huque, M. M.; Islam, M. N.; Hasan, M. Improvement of physico-mechanical properties of jute fiber reinforced polypropylene composites by post-treatment. *Composites, Part A* **2008**, *39*, 1739.

(25) Acar, I.; Pozan, G. S.; Ozgumus, S. Thermal oxidative degradation kinetics and thermal properties of poly(ethylene terephthalate) modified with poly(lactic acid). *J. Appl. Polym. Sci.* **2008**, *109*, 2747.

(26) Paulik, F. Special trends in thermal analysis. *Talanta* **1996**, *43*, 2025.

(27) Zhu, J.; Shao, H.; Hu, X. Morphology structure of electrospun mats from regenerated silk fibroin aqueous solutions with adjusting pH. *Int. J. Biol. Macromol.* **2007**, *41*, 469.

(28) Spinger, V. *Worked examples in X-ray analysis (supplied with the computer controlled XRD)*; Type JDX-11P 3A, JEOL, Japan; Springer: Berlin, 2006.

(29) Singha, A. S.; Kaith, B. S.; Chauhan, A.; Misra, B. N. Mechanical properties of natural fibre reinforced polymer composites. *J. Polym. Mater.* **2006**, *23*, 3456.

(30) Singha, A. S.; Shama, A.; Thakur, V. K. Pressure induced graft-co-polymerization of acrylonitrile onto Saccharum cilliare fibre and evaluation of some properties of grafted fibre. *Bull. Mater. Sci.* **2008**, *31*, 7.

(31) Liu, Z.-T.; Chang'an, S.; Liu, Z.-W.; Jian, L. Adjustable wettability of methyl methacrylate modified ramie fibre. *J. Appl. Polym. Sci.* **2008**, *109* (5), 2888.

(32) Hongehun, L.; Jincai, L.; Yuetao, Z.; Ying, M. Ethylene/a-olefin copolymerization using diphenylcyclopentadienyl-phenoxytitanium dichloride/ $Al(^{i}Bu)_3$/$[Ph_3C][B(C_6F_5)_4]$ catalyst systems. *J. Appl. Polym. Sci.* **2008**, *109*, 3030.

(33) Das, A. M.; Saikia, C. N.; Hussain, S. Grafting of methyl methacrylate (MMA) onto *Antheraea assama* silk fiber. *J. Appl. Polym. Sci.* **2001**, *81*, 2633.

Received for review April 13, 2010
Revised manuscript received November 12, 2010
Accepted December 1, 2010

IE100867G